Research Square

Preprints are preliminary reports that have not undergone peer review.
They should not be considered conclusive, used to inform clinical practice,
or referenced by the media as validated information.

Preparation of 3D Print Scaffolds Fe_3O_4@ Food Oils/Chitosan/Polylactic Acid/Polyurethane Modified Natural Protein Pegylated for Cardiovascular Blood

sholila Naderi
Islamic Azad University North Tehran Branch
Akbar Esmaeili (akbaresmaeili@yahoo.com)
Islamic Azad University North Tehran Branch

Research Article

Keywords: Scaffolds, 3D print, medicine food, polymer, polysaccharides

Posted Date: May 28th, 2021

DOI: https://doi.org/10.21203/rs.3.rs-547203/v1

License: This work is licensed under a Creative Commons Attribution 4.0 International License.
Read Full License

Abstract

Food oils used in 3D polysaccharides modified with natural protein polymer modified polymer scaffolds can help to reduce blood pressure. This study aimed to use food oils as blood pressure-reducing medicine, bind them to magnetic iron nanoparticles, then bind them to polymeric 3D scaffolds (chitosan, polylactic acid and polyurethane), modified with natural protein and finally separate them. This method made it possible to investigate different variables for nanoparticles. In this project, synthesis polymer, food medicinal oils, modified gelatin, PEGylation, food loading and release process in nanocarrier with different concentrations were examined and cell proliferation was optimized. The results show that 75% of the medicine loaded on iron magnetic NPs containing PEGylated polymer scaffolds was released. Cell proliferation was performed for the sample. In this process, modification of scaffolding with polysaccharides modified with natural protein and food oil increased the efficiency of nanoparticles among the studied *Allium sativum* oil and *Zingiber officinale* oils. These behaved very similarly to each other and *A. sativum* had the biggest effect in lowering blood pressure. The application of food medicine oils in 3D mode scaffolding has not been studied before and this is the first analysis to do so, using nanoparticles.

1. Introduction

Today, there is a growing demand for woven vascular engineering, that is effective in the long-term for replacing or bypassing damaged arteries in various cardiovascular diseases. Ideal tissue engineering vessels should be biocompatible, blood compatible, and resistant to the spread of aneurysms, and be easily implantable in the body [1, 2]. Research has shown that scaffolds are made from degenerated natural tissue or biodegradable biopolymers and synthetic polymers to make vascular bonds for tissue engineering. Polysaccharides are biological polymers that play a key role in improving health. Polylactic acid is considered to be one of the most widely used materials in 3D printing. Rapid decomposition in the environment (in just a few years) and use in medical products are among the features of this valuable substance [3]. The use of biocompatible and non-toxic substances chemically improves artificial scaffolds and improves their mechanical properties, which is one of the requirements for the production of ideal vascular grafts [4]. Gelatin is a solid, semi-transparent, and insoluble substance derived from bovine bone or collagen in pig skin, and because of its resemblance to collagen and its biological origin, it has been introduced as an attractive polymer for tissue engineering applications [5]. Ganji et al., [6] used castor oil and polyethylene glycol to produce a plant-based scaffold that was able to produce blood vessels in the animal phase without regurgitation and infection under rabbit skin. Mozumder et al.,[7] studied biomedical applications of polymeric nanobiocomposites. Pourfarhangi et al.,[8] proposed a new way to build a polymer scaffold consisting of a decomposed cell network of the heart for use in cardiac tissue engineering. Khalili and Esmaeili2 were able to synthesize polyurethane for use in tissue engineering. They explained hybrid polymer properties of nanofibers in anticoagulant drugs. O'Brien[9] explained different materials application in scaffolds concerning the tissue engineering field. Tissue engineering with 3D printing can produce and repair damaged tissues engineering by combining cellular

parts of the body with biocompatible materials. An[10] explained that - compared to synthetic polymers – 3D technical natural polymers can provide good biocompatibility for cells. The ability of natural polymers to print in 3D is usually weak so for this reason, indirect 3D printing was created for porous 3D scaffolds. In this project, we tried to replace two food medicine oils (*A. sativum* oil and *Z. officinale* oils) with chemical drugs and connect them to Fe3O4@NPs in the first stage. Then we set out to connect them with polymer 3D scaffolds, and at the end of their PEGylation, ensure their effectiveness in gradually reducing blood pressure. Scheme 1 illustrates the steps for producing Fe3O4@ food medicine oil /CS/PLA/PU-Mo Ge-PEGylated.

2. Materials And Methods

2.1.Materials

All laboratory materials used in this project, including chitosan (CS) (medium molecular weight, 75–85% degree of deacetylation), polylactic acid (PLA) (medium molecular weight), polyurethane (PU) (medium molecular weight), polyethylene glycol (PEG) (low molecular weight, 400), Tween 80 (26 kDa) were purchased from Sigma Chemical Co. Meanwhile, $MnCl_2.4H_2O$ (98%), $FeCl_3.6H_2O$ (98%), NaOH (99%), and glutaraldehyde were bought from Merck Co. Lastly, chloroform (99%) and formic acid (95%) solvents were sourced from Sigma-Aldrich, Germany.

2.2. Synthesis of magnetic iron oxide nanoparticles

307.2 g of hexahydrate of iron chloride, 97.7 g of short-grained iron chloride were dissolved in 100 ml distilled water to make magnetic NPs. The subsequent product was placed in a bathroom sonicator for 30 min, then stirred for 2 h under a stream of nitrogen gas. Concentrated ammonia was used as the precipitating agent. Following the reaction, the sediments were separated by a magnetic separation method with a 1.3 T magnet [and washed with distilled water and ethanol. The sediment was then dried in an oven at 40^0 C.

2.3. Connection of *A. sativum* oil and *Z. officinale* oils to magnetic nanoparticles

In order to take advantage of the antihypertensive properties of medicinal plants, various food oils were used, including olive oil, sesame, coconut, almond, *A. sativum* oil and *Z. officinale* oils, lavender and coriander. In this way, 0.5 g of each of the above oils was mixed with 0.5 g of iron magnetic NPs and the solvent was stirred on a magnetic stirrer for 24 h in the solvent. After this the obtained products were extracted. Fe_3O_4@ *A. sativum* oil and Fe_3O_4@ *Z. officinale* oil formed in the section.

2.4. Preparation of CS/PLA/PU solutions for scaffolding

Polymeric scaffolding was done using solutions with concentrations of 4-8%. The best scaffolding was obtained from a solution of 6% of each, which was prepared from 2 g of polymer in 3.33 ml of formic

acid. In the process Fe_3O_4@ *A. sativum* oil /CS/PLA/PU and Fe_3O_4@ *Z. officinale*/CS/PLA/PU were produced.

2.5. Scaffolding Method

6% solutions of each polymer were scaffolded with a 3D printer and kept at 80^0 C temperature for 10 d. After the solvent dried, they were placed in the freezer for 5 d.

2.6. Stabilization of scaffolding

In order to establish a connection between the molecules, polymer scaffolds were placed in a 2% volumetric GA solution for 4 h. They were then removed from the solution and rinsed with deionized water and finally placed in a freezer for 24 h.

2.7. Placing iron magnetic nanoparticles containing food oils on polymer scaffolds

0.5 g of each of the above extracted products was mixed with 0.5 g of modified polymer 3D scaffold and dissolved in a solvent for 24 h on a magnetic stirrer, after which the obtained products were extracted.

2.8. Modification of scaffolding containing magnetic nanoparticles of iron and medicine by Gelatin

In order to improve the adhesion of the cell to the scaffold's surface and to increase its surface properties for use in tissue engineering, 3D polymer scaffold containing magnetic iron NPs and drug was reacted with gelatin. In this way, 1g from the scaffold was mixed with 0.5 g gelatin in 100 ml water for 24 h and then the resulting sediments were collected. In the process Fe_3O_4@ *A. sativum* oil /CS/PLA/PU modified gelatin and Fe_3O_4@ *Z. officinale*/CS/PLA/PU modified gelatin were produced.

2.9. PEGylation of 3D polymer scaffolding containing magnetic nanoparticles of iron and medicine

To increase the stability and durability of scaffolds in the body, scaffolds were PEGylated. In such a way 0.5 g PEG (400) is dissolved in 100 ml of 98% ethanol (ambient temperature, 300 rpm). This solution is fixed on pH=7.4 by 1 M sodium hydroxide. The scaffolds containing magnetic iron NPs and drug were mixed with this solution and placed at room temperature for 18 h. Then, the PEGylated scaffolds were separated by 1.3T magnet and distilled with water and ethanol washed twice. In the process Fe_3O_4@ *A. sativum* oil /CS/PLA/PU modified gelatin PEGylated (Fe_3O_4@ *A. sativum* oil /CS/PLA/PU-Mo Ge-PEGylated) and Fe_3O_4@ *Z. officinale*/CS/PLA/PU modified gelatin PEGylated (Fe_3O_4@ *Z. officinale*/CS/PLA/PU-Mo Ge-PEGylated) were produced.

2.10. Release of medication

2.10.1. Determining the actual amount of medicine loading

Ultraviolet– visible (UV-Vis) spectroscopy at 275 nm served to determine the actual amount of medicine (garlic oil) loaded on magnetic iron NPs containing PEGylated polymer scaffolds (CS/PLA/PU). 50 mg of

the sample was dissolved in 100 ml of the phosphate buffer pH = 7.4 and stirred for 24 h at room temperature with a magnetic stirrer. Then the product was separated. The actual amount of medicine loaded was calculated by the following equation (Eq. **1**):

$$AC = \left(\frac{Mact}{Mms}\right) \times 100 \qquad (1)$$

Where Mact is the weight of the sample containing medicine, Mms is the weight of the medicine without the sample and AC represents the amount of medicine loaded.

2.10.2. Determination of medicine releaseprofile

40 mg of the sample was dissolved in 100 ml of phosphate buffer solution with pH = 7.4 and stirred at room temperature with a magnetic stirrer. With a certain time, interval of up to 48 h, 5 ml from the top solution was removed and the sediments in it were separated. Then its absorption was read by a UV-Vis device at 275 nm and the amount of medicine was obtained from the calibration curve. The medicine cumulative percentage was calculated from the following equation (Eq. 2):

$$cumulative\ release\ rate = \sum_{t=0}^{t} \frac{Mt}{M0} \times 100 \qquad (2)$$

Where t is the medicine release time, Mt is the cumulative amount of medicine in time unit and M0 is the initial amount of medicine in the sample. The results show that 75% of the medicine loaded on iron magnetic NPs containing PEGylated polymer scaffolds (CS/PLA/PU) was released.

3. Results And Discussion

3.1. FT-IR analysis

FT-IR analysis helped to characterize chemical interaction of iron magnetic NPs connected *A. sativum* oil and *Z. officinale* oil, after connecting with polymeric scaffolds (CS/PLA/PU), and after the PEGylation, in the 400–4000 cm^{-1} range (see **Figure 1**). FT-IR spectrum of iron magnetic NPs connected to *A. sativum* oil (**Figure 1A**), after connecting with polymeric scaffolds (CS/PLA/PU) (**Figure 1B**), and after the PEGylation (Fe_3O_4@ *A. sativum* oil /CS/PLA/PU-Mo Ge-PEGylated) (**Figure 1C**), identified the chemical absorption (**Figure 1**). FT-IR spectrum of iron magnetic NPs connected to *Z. officinale* oil (**Figure 1D**), after connecting with polymeric scaffolds (Cs/PLA/PU) (**Figure 1E**), and after the PEGylation (Fe_3O_4@ *Z. officinale* oil /CS/PLA/PU-Mo Ge-PEGylated) (**Figure 1F**), identified the chemical absorption (**Figure 1**). The results show that the *A. sativum* oil and *Z. officinale* oil exhibited the closest behavior to other food oils (**Figure 1**). In **Figure 1A** and **D**, the signal of iron magnetic NPs is seen at 500 cm^{-1}. The specific peaks at 476 and 578 cm^{-1} may be due to O-Fe stretching vibration and 1645 cm^{-1} is related to H_2O deformation, respectively [11]. In **Figure 1B** and **E**, the strong signals of PLA and CS (C=O, C–O) are evident at 1560 cm^{-1} while the signal of PU (C–H, C–O) is seen at 1340 cm–1 [3]. Furthermore, a broad

signal related to the food medicine garlic can be seen at 3000 cm^{-1}. Signals of the N–H and O–H bonds exist at 3000 cm^{-1}[2]. To confirm coating polymers on Fe_2O_4 NPs containing oil, broad absorption peaks at 3394 and 3417 cm^{-1} belong to the OH group of polymers. Absorption at 1617 cm^{-1} is due to the stretching vibrations C=O of polymers. In **Figure 1C**, a strong signal at 1100 cm^{-1} is observed and it is related to the C–O–C bond of ethylene glycol. 3411 and 3382 cm^{-1} OH concerning the PEGylated polymers [12].

Figure 1. Comparison of the FT-IR spectra of (**A**) Fe_3O_4@ *A. sativum* oil (**B**) Fe_3O_4@ *A. sativum* oil /CS/PLA/PU; (**C**) Fe_3O_4@ *A. sativum* oil /CS/PLA/PU-Mo Ge-PEGylated; (**D**) Fe_3O_4@ *Z. officinale* oil; (**E**) Fe_3O_4@ *Z. officinale* oil/CS/PLA/PU; (**F**) Fe_3O_4@ *Z. officinale* oil /CS/PLA/PU-Mo Ge-PEGylated.

3.2. XRD analysis

In order to evaluate suitable particle size and morphology, we used XRD analysis to confirm the results with SEM images. **Figure 2A** and **2B** illustrate the crystalline structure of prepared Fe_3O_4@ *A. sativum* oil /CS/PLA/PU-Mo Ge-PEGylated and Fe_3O_4@ *Z. officinale*/CS/PLA/PU-Mo Ge-PEGylated, which were confirmed by XRD analysis. The diffraction peaks are related to the particles' crystal structure in the angle range of ($1 < 2\theta < 80$). Comparison of the XRD patterns of two *A. sativum* oil and *Z. officinale* oil in the **Figure 2A** and **2B** indicates the most obvious changes in the XRD pattern of *A. sativum* oil (**Figure 2A**). The average crystalline size was obtained from X-ray diffraction data using Scherrer's formula:

$$D = \frac{K\lambda}{\beta \cos\theta} \qquad (3)$$

Where k=0.94, λ=0.154056 nm, and β is the full width at half maximum in radians [13,14]. XRD pattern of Fe_3O_4@ *A. sativum* oil [**Figure 2A(a)**], after Fe_3O_4@ *A. sativum* oil /CS/PLA/PU [**Figure 2A(b)**], and Fe_3O_4@ *A. sativum* oil /CS/PLA/PU-Mo Ge-PEGylated [**Figure 2A(c)**, is show in **Figure 2A**. The XRD patterns reveal signals at 14 to 30 and these are related to polymers so it agrees with what previous studies have documented [15]. The results show that the two *A. sativum* oil and *Z. officinale* oil indicate the closest behavior to other oils. Of these, *A. sativum* oil shows the most obvious changes (**Figure 2A** and **2B**). In **Figure 2A**, which refers to the XRD analysis of the sample containing *A. sativum* oil, it clearly shows the changes in increasing both the NPs and polymers, and PEGylating the sample (**Figure 2A**). The XRD patterns exhibited peaks corresponding to Fe_3O_4, marked with their indices (250), (355), (370), (454), (522) and (575), which are similar to those reported before for Fe3O4 NPs [16]. The XRD of patterns showed signals at 14 to 30, related to polymers and this echoes previous studies [15]. The XRD patterns exhibited peaks corresponding to Fe_3O_4@ *Z. officinale* oil/CS/PLA/PU, marked with their indices (220), (311), (400), (422), (511) and (440), which are similar to those reported previously for Cs-Fe_3O_4 -NPs, and marked with 2θ=16-29 and 2θ= 19, 20. These are similar to those reported before for PLA and PU, respectively [2]. **Figure 2B(a)** show XRD of patterns showed signals at 19 and 23, related to polyethylene glycol, after PEGylation, which is similar to previous studies [17]. XRD pattern of Fe_3O_4@ *Z. officinale* oil

[**Figure 2B(a)**], after Fe_3O_4@ *Z. officinale* oil/CS/PLA/PU [**Figure 2B(b]**, and Fe_3O_4@ *Z. officinale*/CS/PLA/PU-Mo Ge-PEGylated [**Figure 2B(c)**], is shown in **Figure 2B**.

Figure 2B(a) show XRD patterns exhibited peaks corresponding to Fe_3O_4, marked with their indices (250), (355), (370), (454), (522) and (575), which are similar to those reported before for Fe3O4 NPs [18,19]. The XRD of patterns showed signals at 14 to 30, related to polymers as indicated in other studies [20]. **Figure 2B(b)** show XRD patterns exhibited peaks corresponding to Fe_3O_4@ *Z. officinale*/CS/PLA/PU, marked with their indices (220), (311), (400), (422), (511) and (440), which are similar to those reported before for Cs-Fe_3O_4 NPs, and marked with 2θ= 16-29 and 2θ= 19, 20 which are similar to those reported before for PLA and PU, respectively [21]. **Figure 2B(c)** show XRD of patterns revealed signals at 19 and 23, related to polyethylene glycol, after PEGylation, which is similar to previous studies [17]. The results show that *A. sativum* oil and *Z. officinale* oil behave very similarly to other food oils and among these, *A. sativum* oil shows the most obvious changes (**Figure 2B(b)** and **Figure 2B(c)**). In **Figure 2A**, which illustrates the XRD analysis of the sample containing *A. sativum* oil, it clearly depicts the changes involved in: firstly, increasing the NPS and the polymers; and secondly, PEGylating the sample.

3.3. SEM analysis

Morphological analysis was undertaken with the help of electron microscopic images. **Figure 3A-C** shows the SEM images of the samples. **Figure 3A** relates to Fe_3O_4@ *A. sativum* oil and **Figure 3B** illustrates the combination of Fe_3O_4@ *A. sativum* oil/CS/PLA/PU. **Figure 3C** corresponds to the combination Fe_3O_4@ *A. sativum* oil /CS/PLA/PU-Mo Ge-PEGylated. In the SEM image of iron magnetic NPs connected to Fe_3O_4@ *A. sativum* oil, it can be seen clearly that the particles are uniformly aggregated, spherical shaped with a size of 6–30 nm [22]. **Figure 3B** shows the SEM image of Fe_3O_4@ *A. sativum* oil /CS/PLA/PU-Mo Ge-PEGylated, and it can be seen clearly that the particles are uniformly aggregated, spherical shaped with a size of 50-350 µm [2], [23,24]. **Figure 3B** shows the PEGylation of the 3D polymers (CS/PLA/PU) attached to the magnetic iron NPs containing the gelatin-coated *A. sativum* oil. In this study we attempted to examine the image with an electronic microscope. Since the sample was very thick and oily and did not dry completely even under vacuum, we had to dissolve it in a little methanol and then take a picture of it. Measurement of the sample when using scanning electron microscopy (SEM) revealed that the sample was 100 to 135 nm in size.

3.4. ZPS analysis

The particle has a surface charge inside the fluid, and an increase in the concentration of ions with the opposite charge to the surface of the particle is always seen around the surface of the particle inside the fluid. Thus, an additional layer of these ions surrounds the surface of the particle and forms an additional layer around the particle. When a particle moves in a fluid, the surrounding layer also moves with the particle and moves with the particle, and it can be assumed that a hypothetical distance between the particle and the fluid environment is the hypothetical distance of the extra layer that surrounds the particle. This distance is called the hydrodynamic distance and the potential at this distance is known as

the zeta potential. In fact, the zeta potential is a parameter for the potential stability of the colloidal system. If all the particles in the suspension are negatively or positively charged, the particles tend to repel each other and show no tendency to coalesce.

The tendency of particles to repel each other is directly related to the zeta potential. In general, the limit of the suspension's stability and instability can be determined in terms of zeta potential.Show more Esmaeili and Khodaei [25] reported the negative ZPS of PU. They showed PU can be used as a conductive solution in the double-needled electrospinning method. The negative charge of the PU surface led to a better conduction of ions in the electrospinning device. It also caused better blood compatibility with PU than other polymers. They showed that the negative and positive numbers obtained can be effective in clinical tests [3]. So, we decided to do this test on our sample that contained the three polymers (CS/PLA/PU). The results show that the zeta potential is -1.29 mV, the zeta deviation is 0 mV and the ion conductivity is 13.3 ms/cm.Show more

3.5. MTT analysis

In order to evaluate the survival of human fibroblast cells under the influence of drugs, MTT test was undertaken. Therefore, human fibroblast cells were cultured in appropriate numbers for this test in 24 h. The cells were then treated with a range of drug concentrations in triplicate.
After reading the final absorption by ELISA reader, it was considered to be 100% and other samples were weighed against it. Esmaeili and Hormozi [26] synthesized magnetic NPs of albumin with organic compounds for absorbing and releasing doxorubicin hydrochloride and then investigated the toxicity of NPs by MTT test. Esmaeili and Khalili [3] prepared a scaffold made of CS//PVA/PU/PANI/*Zingiber officinal* and (CS//PVA/PU/PANI/ heparin) with double-needle electrospinning. It contained anticoagulant drugs and we then examined its toxicity using a MTT test.

3.6. Assessing the effect of toxicity with MTT test

The MTT assay is used to evaluate the bioavailability of cells. The intensity of the purple dye produced is directly proportional to the number of cells that are metabolically active. An appropriate number of cells were cultured in the desired cells from a 96-cell plate with a final volume of 200 µl of serum medium. The plate is incubated for 24 h so that the cells adhere to the surface of the plate. An appropriate amount of medicine was poured into each well. Each concentration was tested in triplicate. After the desired time, the wells were completely emptied and 180 µl of culture medium and 20 µl of MTT solution were added to each well. The plate was wrapped in foil and placed in an incubator at 37 °C for 4 h. The medium was removed from the wells and 200 µl of DMSO was added to each well. After 10 min, the light absorption of the samples was read at 570 nm. In this study, MTT assay was performed for cancer cells as well as normal cells within 24 h after treatment with the test groups. **Table 1** shows the results of light absorption of the studied groups for MTT solution in a period of 24 h. Each drug concentration was repeated three times. The results show that the drug used in 5 concentrations is not significantly different from the control group without the drug and the combination does not show a cytotoxic effect.

Table 1. Light absorption of the 4 groups for MTT solution in a period of 24 h. Each drug concentration was repeated three times.

Concentration	1	2	3	control group
1.2048	0.881	0.784	0.891	0.861
1.1024	0.799	0.751	0.85	0.747
1.512	0.645	0.708	0.612	0.824
1.256	0.202	0.215	0.232	0.791
1.128	0.006	0.005	0.025	0.822

Conclusion

The aim of this study was to use food medicine oil as a blood pressure-reducing medicine. The polymeric 3D print concerned the scaffolds process (Fe_3O_4@ food medicine oil /CS/PLA/PU-Mo Ge-PEGylated). UV-Vis, FT-IR spectra, ZPS, XRD, SEM, MTT test served to determine the data. The results show that 75% of the medicine loaded on iron magnetic NPs containing PEGylated polymer scaffolds was released. Finally, the product obtained was PEGylated and this increased its durability and stability. The best results were obtained at pH = 7.4. This examination show 3D print in the scaffolds process can be more effective for the drug delivery system. It is suggested that future research could investigate industrial synthesis with food medicinal oils for scaffolds.

Abbreviations

Chitosan (CS), Fe_3O_4@nanoparticles (Fe_3O_4@NPs), gelatin (Ge), glutaraldehyde (GA), polylactic acid (PLA), polyurethane (PU), polyethylene glycol (PEG).

Declarations

Conflict of interest

The authors have declared that there is no conflict of interest.

References

1. Rajabi A, Esmaeili A (2020) Preparation of three-phase nanocomposite antimicrobial scaffold BCP/Gelatin/45S5 glass with drug vancomycin and BMP-2 loading for bone regeneration. Colloids

and Surfaces A: Physicochemical and Engineering Aspects 606:125508

2. Esmaeili A, Khodaei M (2019) A new and enzymatic targeted magnetic macromolecular nanodrug system which delivers methadone and rifampin simultaneously. ACS Biomaterials Science & Engineering
3. Amand FK, Esmaeili A (2020) Investigating the properties of electrospun nanofibers made of hybride polymer containing anticoagulant drugs. Carbohydrate polymers 228:115397
4. Martin V, Ribeiro IA, Alves MM, Gonçalves L, Claudio RA, Grenho L, Fernandes MH, Gomes P, Santos CF, Bettencourt AF (2019) Engineering a multifunctional 3D-printed PLA-collagen-minocycline-nanoHydroxyapatite scaffold with combined antimicrobial and osteogenic effects for bone regeneration. Materials Science and Engineering: C 101:15-26
5. Esmaeili A, Afshari S, Esmaeili D (2015) Formation of harmful compounds in biotransformation of lilial by microorganisms isolated from human skin. Pharm Biol 53 (12):1768-1773. doi:10.3109/13880209.2015.1005755
6. Ganji Y, Kasra M, Kordestani SS, Hariri MB (2014) Synthesis and characterization of gold nanotube/nanowire–polyurethane composite based on castor oil and polyethylene glycol. Materials Science and Engineering: C 42:341-349
7. Mozumder MS, Mairpady A, Mourad AHI (2017) Polymeric nanobiocomposites for biomedical applications. Journal of Biomedical Materials Research Part B: Applied Biomaterials 105 (5):1241-1259
8. Pourfarhangi KE, Mashayekhan S, Asl SG, Hajebrahimi Z (2018) Construction of scaffolds composed of acellular cardiac extracellular matrix for myocardial tissue engineering. Biologicals 53:10-18
9. O'brien FJ (2011) Biomaterials & scaffolds for tissue engineering. Materials today 14 (3):88-95
10. An J, Teoh JEM, Suntornnond R, Chua CK (2015) Design and 3D printing of scaffolds and tissues. Engineering 1 (2):261-268
11. Esmaeili A, Ghobadianpour S (2016) Antibacterial activity of Carum copticum extract loaded MnFe2O4 nanoparticles coated with PEGylated chitosan. Industrial Crops and Products 91:44-48
12. Şentürk SB, Kahraman D, Alkan C, Gökçe İ (2011) Biodegradable PEG/cellulose, PEG/agarose and PEG/chitosan blends as shape stabilized phase change materials for latent heat energy storage. Carbohydrate Polymers 84 (1):141-144
13. Bindhu M, Umadevi M (2013) Synthesis of monodispersed silver nanoparticles using Hibiscus cannabinus leaf extract and its antimicrobial activity. Spectrochimica Acta Part A: Molecular and Biomolecular Spectroscopy 101:184-190
14. Tadayon A, Jamshidi R, Esmaeili A (2015) Delivery of tissue plasminogen activator and streptokinase magnetic nanoparticles to target vascular diseases. Int J Pharm 495 (1):428-438. doi:10.1016/j.ijpharm.2015.09.008
15. Yavuz AG, Uygun A, Bhethanabotla VR (2010) Preparation of substituted polyaniline/chitosan composites by in situ electropolymerization and their application to glucose sensing. Carbohydrate

Polymers 81 (3):712-719

16. Baraton M-I, Chen X, Gonsalves KE (1996) Application of Fourier Transform Infrared Spectroscopy to Nanostructured Materials Surface Characterization: Study of an Aluminum Nitride Powder Prepared via Chemical Synthesis. In. ACS Publications,
17. Barron MK, Young TJ, Johnston KP, Williams RO (2003) Investigation of processing parameters of spray freezing into liquid to prepare polyethylene glycol polymeric particles for drug delivery. Aaps Pharmscitech 4 (2):1-13
18. Gong FF, Li H, Wang W, Huang J, Xia DD, Liao J, Wu M, Papavassiliou DV (2019) Scalable, eco-friendly and ultrafast solar steam generators based on one-step melamine-derived carbon sponges toward water purification. Nano Energy 58:322-330
19. Masoumi F, Khadivinia E, Alidoust L, Mansourinejad Z, Shahryari S, Safaei M, Mousavi A, Salmanian A-H, Zahiri HS, Vali H (2016) Nickel and lead biosorption by Curtobacterium sp. FM01, an indigenous bacterium isolated from farmland soils of northeast Iran. Journal of environmental chemical engineering 4 (1):950-957
20. Masoumi S, Esmaeili A (2020) In vivo, in vitro, and antibacterial activity of Fe 3 O 4@ RIF-BUP-CMCs-modified by fatty acids nanoparticles to remove drug liver toxins. Applied Nanoscience 10 (11):4149-4160
21. Masoumi S, Esmaeili A (2020) New method of creating hybrid of buprenorphine loaded rifampin/polyethylene glycol/alginate nanoparticles. International Journal of Biological Macromolecules
22. Ma P, Luo Q, Chen J, Gan Y, Du J, Ding S, Xi Z, Yang X (2012) Intraperitoneal injection of magnetic Fe3O4-nanoparticle induces hepatic and renal tissue injury via oxidative stress in mice. International journal of nanomedicine 7:4809
23. Kumar S, Koh J (2012) Physiochemical, optical and biological activity of chitosan-chromone derivative for biomedical applications. International journal of molecular sciences 13 (5):6102-6116
24. Barczewski M, Matykiewicz D, Krygier A, Andrzejewski J, Skórczewska K (2018) Characterization of poly (lactic acid) biocomposites filled with chestnut shell waste. Journal of Material Cycles and Waste Management 20 (2):914-924
25. Esmaeili A, Khodaei M (2018) Encapsulation of rifampin in a polymeric layer-by-layer structure for drug delivery. Journal of Biomedical Materials Research Part A 106 (4):905-913
26. Hormozi N, Esmaeili A (2019) Synthesis and correction of albumin magnetic nanoparticles with organic compounds for absorbing and releasing doxorubicin hydrochloride. Colloids Surf B Biointerfaces 182:110368. doi:10.1016/j.colsurfb.2019.110368

Figures

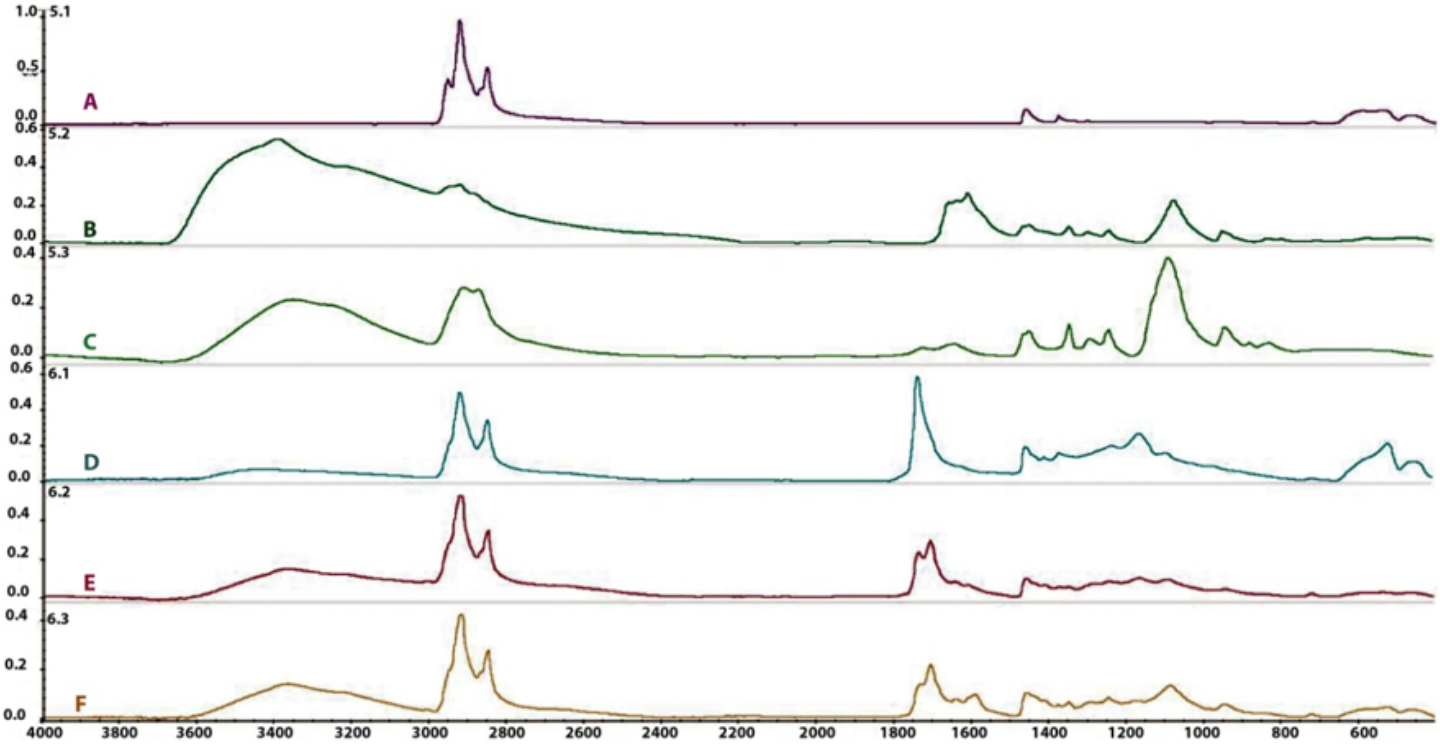

Figure 1

Comparison of the FT-IR spectra of (A) Fe3O4@ A. sativum oil (B) Fe3O4@ A. sativum oil /CS/PLA/PU; (C) Fe3O4@ A. sativum oil /CS/PLA/PU-Mo Ge-PEGylated; (D) Fe3O4@ Z. officinale oil; (E) Fe3O4@ Z. officinale oil/CS/PLA/PU; (F) Fe3O4@ Z. officinale oil /CS/PLA/PU-Mo Ge-PEGylated.

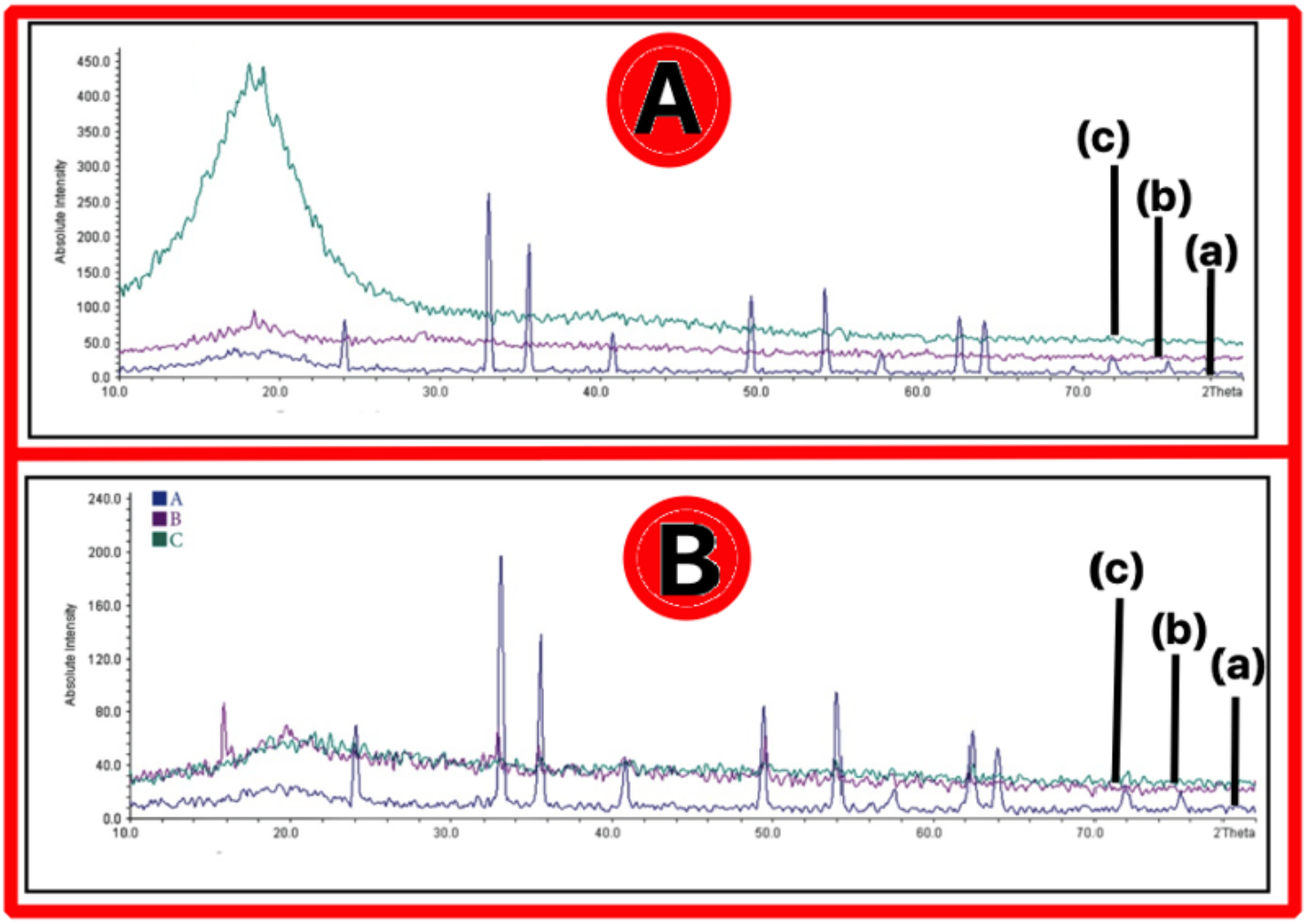

Figure 2

XRD pattern of (A) (a) Fe3O4@ A. sativum oil (b) Fe3O4@ A. sativum oil/CS/PLA/PU; (c) Fe3O4@ A. sativum oil /CS/PLA/PU-Mo Ge-PEGylated; (B) (a) Fe3O4@ Z. officinale oil (b) Fe3O4@ Z. officinale oil /CS/PLA/PU; (c) Fe3O4@ Z. officinale oil/CS/PLA/PU-Mo Ge-PEGylated.

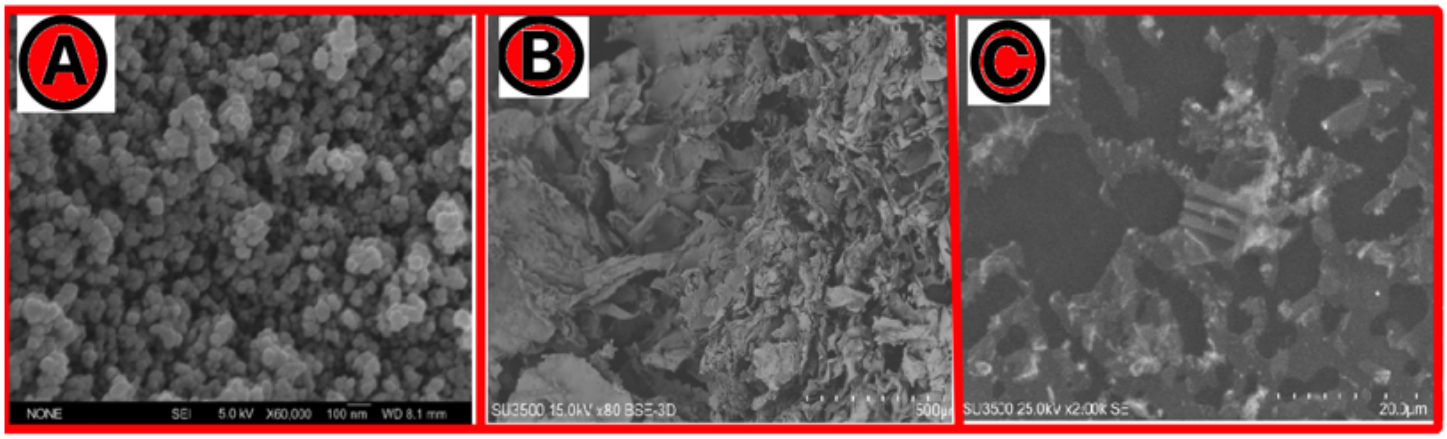

Figure 3

SEM pattern of (A) Fe3O4@ A. sativum oil; (B) Fe3O4@ A. sativum oil/CS/PLA/PU; (C) Fe3O4@ A. sativum oil /CS/PLA/PU-Mo Ge-PEGylated.

Supplementary Files

This is a list of supplementary files associated with this preprint. Click to download.

- schema.png